Journal of Medicinal Chemistry

Brief Article

pubs.acs.org/jmc

Potent HGF/c-Met Axis Inhibitors from *Eucalyptus globulus*: the Coupling of Phloroglucinol and Sesquiterpenoid Is Essential for the Activity

Sheng-Ping Yang,[†,§] Xiao-Wei Zhang,[†,§] Jing Ai,[†,§] Li-She Gan,[‡] Jin-Biao Xu,[†] Ying Wang,[†] Zu-Shang Su,[†] Lu Wang,[†] Jian Ding,[†] Mei-Yu Geng,*[,†] and Jian-Min Yue*[,†]

[†]State Key Laboratory of Drug Research, Shanghai Institute of Materia Medica, Chinese Academy of Sciences, 555 Zu Chong Zhi Road, Zhangjiang Hi-Tech Park, Shanghai, 201203, People's Republic of China

[‡]Institute of Modern Chinese Medicine, College of Pharmaceutical Sciences, Zhejiang University, Hangzhou 310058, People's Republic of China

Supporting Information

ABSTRACT: Eucalyptin A (**1**), together with two known compounds **2** and **3** exhibiting potent inhibition on HGF/c-Met axis, was discovered from the fruits of *Eucalyptus globulus*. **1** possessed an unprecedented carbon framework of phloroglucinol-coupled sesquiterpenoid, and its structure was elucidated by spectroscopic method and ECD calculation. A brief structure−activity relationship discussion indicated that the coupling of a phloroglucinol and a sesquiterpenoid is essential for the activity.

INTRODUCTION

The c-Met tyrosine kinase is a cell surface receptor that is activated by a pleiotropic cytokine hepatocyte growth factor (HGF) and in turn conveys a unique combination of pro-migratory, anti-apoptotic, and mitogenic signals.[1] The aberration of HGF/c-Met axis has been implicated in a variety of human malignancies. HGF/c-Met axis is known to play an important role in regulating cancer invasive growth by coordinating multiple steps involved in this event, including scattering, migration, invasion, and branching morphogenesis.[2] In addition, this axis can activate urokinase plasminogen activator (uPA, urokinase), which promotes extracellular matrix degradation and provokes cancer cell invasion. Given the important role of HGF/c-Met signaling in cancer progression and metastases, this signaling axis has emerged as one of the most promising therapeutic targets in anticancer drugs discovery.

The plant *Eucalyptus globulus* Labill growing widely in the southwest of China has been used as a folk medicine to treat flu, dysentery, eczema, scald, and rheumatism.[3] A preliminary study on this plant in our group has led to the isolation of the three compounds eucalyptals A−C.[4] In a bioactive-guided isolation for HGF/c-Met axis inhibitors, one fraction of the ethanolic extract of the fruits of *E. globulus* showed remarkable inhibitory activity. This fraction was thus subjected to extensive purification to afford the three major compounds **1**−**3**, and **1** was identified as a new structure, namely eucalyptin A. Further biological tests verified that compounds **1**−**3** were responsible for the potent inhibition of the HGF/c-Met axis. Compound **1** was identified as a phloroglucinol-coupled sesquiterpenoid with an unprecedented carbon framework formed by linking the sesquiterpenoid to the C-7′ of phloroglucinol motif. With rare exceptions, the sesquiterpenoid moieties of this compound category reported previously were connected to the C-9′ of phloroglucinol part, e.g., compounds **1** and **2**.[5] Phloroglucinol-coupled sesquiterpenoids, which are found mainly in the *Eucalyptus* genus,[3] exhibited a wide spectrum of significant biological activities, such as HIV-RTase inhibition,[6] granulation inhibition,[7] and antimicrobial effects.[8] The mode-of-action study showed that **1** inhibited HGF-induced c-Met phosphorylation and suppressed HGF-stimulated cell motility and the subsequent invasive behaviors. The novel structural architecture with potent HGF/c-Met axis inhibitory activity of **1**, as well as compounds **2** and **3** with similar effects, provides a great opportunity for the development of a new class of HGF/c-Met axis inhibitor. For the structure−activity relationship (SAR) study, two sesquiterpenoids **4** and **5**, and two phloroglucinol analogues **6** and **7** were included and tested for HGF/c-Met axis inhibition. Compounds **4**−**7** were also isolated from *E. globulus* in this study and are believed to be the precursors of compounds **1**−**3**. Observation of the structures and activities of compounds **1**−**7** clearly indicated that the coupling of a phloroglucinol and a sesquiterpenoid is essential for the activity. Herein, we report the isolation and structural elucidation of compound **1** and, in particular, the potent inhibitory activity of HGF/c-Met axis and the brief SAR study of this compound class.

RESULTS AND DISCUSSION

Eucalyptin A (**1**) (Figure 1) was obtained as an optically active ($[\alpha]_D^{20}$ −80.7) amorphous powder. Its molecular formula was established as $C_{28}H_{40}O_6$ by the HREIMS ion at m/z 472.2853 ($[M]^+$, calcd 472.2825) requiring 9 degrees of unsaturation. The positive ESIMS ion at m/z 495.2 $[M + Na]^+$ and the negative ESIMS ion at m/z 471.3 $[M - H]^-$ further secured the assignment of molecular formula. The IR spectrum of **1** implied the presences of carbonyls (1616 cm^{-1}) and hydroxyls (3425

Received: May 30, 2012
Published: August 30, 2012

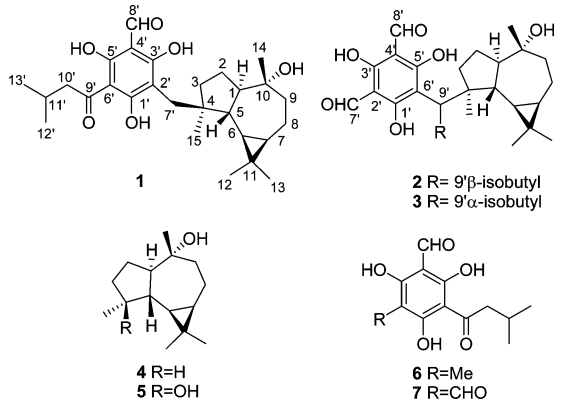

Figure 1. Structures of **1** and the related compounds.

cm^{-1}). In its ^{13}C NMR spectrum, 28 carbon resonances were observed and were further classified by HSQC and DEPT experiments as six methyls (δ_C 16.8, 18.4, 20.2, 22.7, 22.7, and 28.9), six methylenes, five methines, three sp^3 quaternary carbons (δ_C 19.3, 46.8, and 75.8), one ketone (δ_C 206.5), one aldehyde (δ_C 192.0), and a persubstituted benzene (δ_C 103.4, 104.1, 104.6, 162.2, 168.0, and 172.7). These functionalities accounted for 6 degrees of unsaturation, and the remaining 3 degrees of unsaturation required the presence of three additional rings in **1**. The aforementioned data suggested that compound **1** is a phloroglucinol-coupled sesquiterpenoid.

Comparison of the ^{1}H and ^{13}C NMR data of **1** with those of grandinol (**6**),[9] macrocarpal A (**2**),[5] and euglobals T1 and IIc[10] indicated the presence of a grandinol moiety (Figure 2,

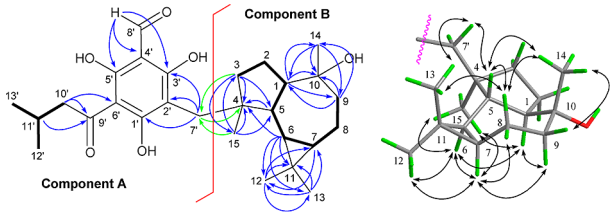

Figure 2. ^{1}H−^{1}H COSY (−), key HMBC (H→C), and key ROESY (H↔H) correlations of **1**.

component A), and this was further confirmed by ^{1}H−^{1}H COSY and HMBC spectra (Figure 2), in which the HMBC correlations of H-10′ and H-11′/C-9′ (δ_C 206.5) and H-10′/C-6′ (δ_C 103.4) allowed the attachment of the 3-methylbutanoyl to C-6′. The key HMBC correlations of H-8′/C-3′ (δ_C 162.2), C-4′ (δ_C 104.1) and C-5′ (δ_C 168.0), and H-7′/C-1′ (δ_C 172.7), C-2′, and C-3′ located the aldehyde and the C-7′ methylene to C-4′ and C-2′, respectively, and also allowed the assignment of three hydroxyls at C-1′, C-3′, and C-5′. A sesquiterpenoid moiety (Figure 2, component B) composed of the remaining 15 carbons was subsequently established by a comprehensive analysis of NMR spectra. After the assignment of all protons to their bonding carbons by HSQC spectrum, a proton bearing spin coupling unit as drawn with bold bonds in the component B was readily outlined by ^{1}H−^{1}H COSY spectrum. The connections of this proton bearing subunit with the other fragments were also achieved by the HMBC experiment. In the HMBC (Figure 2), the correlations from H_2-3, H-5, and H_3-15 to C-4 attached C-3, C-5, and C-15 to the quaternary carbon of C-4 to furnish a five-membered ring; the correlation networks of H-6, H-7, and H_3-12 (13)/C-11, H-6 and H-7/C-12 (13), and H_3-12 (13)/C-6 (7) established the cyclopropane and also located Me-12 and Me-13 to C-11; the mutual correlations of H-1, H_2-9 and H_3-14/C-10 (δ_C 75.8), H-1 and H_2-9/C-14, and H_3-14/C-1 and C-9 allowed the attachment of C-1, C-9, and C-14 to C-10 to furnish the seven-membered ring and also placed a hydroxyl at the oxygenated quaternary C-10. In the ROESY spectrum (Figure 2), the correlations of CH_3-12/H-6, CH_3-12/H-7, H-6/H-7, H-6/CH_3-15, CH_3-15/H-7, H-7/H-8α, H-7/H-9α, H-9α/H-1, H-1/H-6, and H-1/CH_3-15 indicated that they were cofacial and were arbitrarily assigned to be α-oriented. Subsequently, the ROESY cross-peaks of CH_3-13/H-8β, H-8β/H-5, H-8β/CH_3-14, CH_3-14/H-5, and CH_3-14/H-9β revealed that H-5, H-8, CH_3-13, and CH_3-14 were in a β-orientation, respectively. The ^{1}H and ^{13}C NMR data of component B showed high similarity to those of macrocarpal A (**2**),[5,11] an aromadendrane-type sesquiterpenoid, further supporting this assignment. The assembly of components A and B in **1** was made by the key HMBC correlations of H_2-7′/C-4 and H_3-15/C-7′. The structure and relative stereochemistry of **1** was thus established.

To establish its absolute configuration, the CD spectrum of **1** was measured in CH_3OH (Figure 3). However, its CD

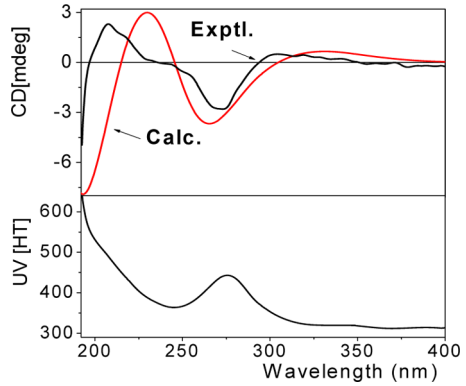

Figure 3. B3LYP/6-31++G(2d,2p)//B3LYP/6-31+G(d) calculated ECD (red) (σ = 0.4 eV) and experimental ECD spectra (black) of **1**.

spectrum did not provide reliable exciton coupling to assign the absolute structure directly, and there were also no proper model compounds available for reference to solve this matter. The calculation of electronic circular dichroism (ECD) by using time-dependent density functional theory (TDDFT)[12] was thus applied in combination with the experimental CD data to establish the absolute configuration of **1**. The calculated ECD in gas phase (for the detailed calculation, see Supporting Information (SI)) of **1** matches very well with the experimental ECD (in CH_3OH) in the region of 200−400 nm (Figure 3), in which the experimental ECD showed positive (304 nm, weak), negative (273 nm, strong), and positive (208 nm, strong) Cotton effects, and the calculated ECD gave positive (328 nm, weak), negative (265 nm, strong), and positive (230 nm, strong) Cotton effects. The absolute configuration of **1** was thus assigned as depicted.

Six known compounds were identified as macrocarpal A (**2**),[5] M−B (**3**),[6] globulol (**4**),[13] 10α-dihydroxyaromadendrane (**5**),[14] grandinol (**6**),[9] and jensenone (**7**)[15] on the basis of spectroscopic data.

Compound 1 Blocks HGF/c-Met Axis Signaling Pathway. To study the effects of **1** on the HGF/c-Met axis, we first used four kinds of cell lines, MDCK, A549, NCI-H441, and

dx.doi.org/10.1021/jm3007454 | J. Med. Chem. 2012, 55, 8183−8187

DU145, which naturally express c-Met and respond to HGF stimulation as well. We found that **1** markedly inhibited HGF-induced c-Met phosphorylation in a dose-dependent manner, and over 50% inhibition was observed at the dosage of 5 μM in all tested cell lines (Figure 4A–D), suggesting that **1** inhibited

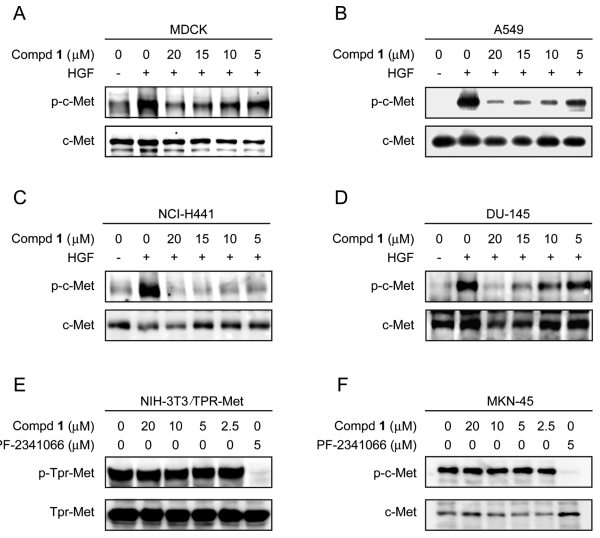

Figure 4. **1** inhibited HGF-induced c-Met phosphorylation. (A–D) **1** suppressed c-Met phosphorylation stimulated by HGF in MDCK cells (A), A549 cells (B), NCI-H441 cells (C), and DU-145 cells (D). (E) **1** failed to inhibit TPR-Met phosphorylation in NIH-3T3/TPR-Met cells. (F) **1** failed to inhibit c-Met phosphorylation in MKN-45 cells.

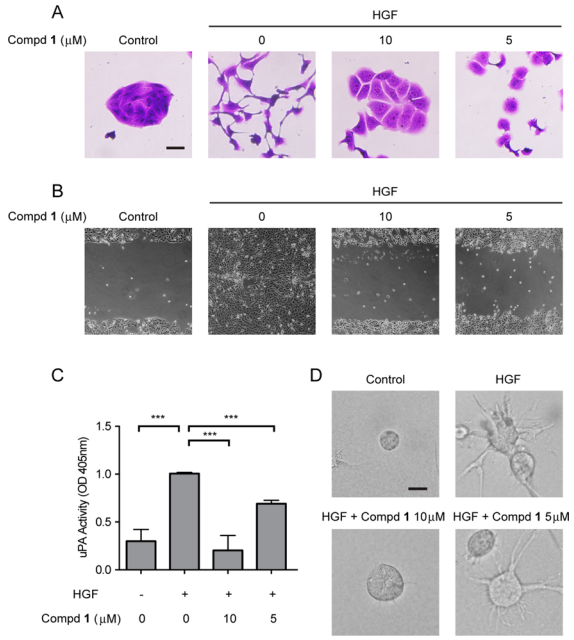

Figure 5. **1** strongly inhibited HGF-stimulated cell metastatic phenotype in vitro. (A) **1** inhibits HGF-induced cell scattering in MDCK cells (scale bars, 50 μm). (B) **1** suppressed HGF-induced cell migration of MDCK cells using wound-healing assay. (C) **1** reduced HGF-induced urokinase activity in MDCK cells. (D) **1** impaired HGF-induced MDCK cell branching morphogenesis on collagen (scale bars, 50 μm). Data from three independent experiments performed in triplicate are presented as mean ± SD ***, $P < 0.001$.

HGF/c-Met axis. Because c-Met can be activated through an HGF-dependent or HGF-independent manner, we further determined whether the inhibition of c-Met phosphorylation by **1** depends on HGF or not. To this end, we extended our study to genetically generated NIH-3T3 cell line that stably express a constitutively active oncogenic version of c-Met, designated as NIH-3T3/TPR-Met cells, and MKN-45 cancer cell line naturally displaying a *MET* amplification driven cell growth. The results showed that **1**, even at the concentration of 20 μM, failed to inhibit c-Met phosphorylation in these two cell lines (Figure 4E,F), indicating that the inhibition of **1** on HGF/c-Met axis signaling is HGF dependent. Moreover, **1** showed no direct inhibitory effect on c-Met kinase activity in cell-free system using Met kinase-based ELISA assay (IC_{50} > 50 μM), further supporting this notion. All these data showed that the inhibition of c-Met activation by the compound depends on the HGF stimulation, which indicated that **1** is likely an antagonist of HGF or blocks the extracellular domain of c-Met.

1 Inhibits HGF-Induced Cell Scattering. Activated HGF/c-Met signaling is known to promote cell scattering, a hallmark of cancer invasiveness and metastasis. It has been well documented that MDCK cells, which normally grow in clusters, exhibit disruption and scattering of cell colonies upon HGF stimulation. To determine the effect of **1** on cell scattering behavior, MDCK cells were treated with HGF in the presence or the absence of the agent. As shown in Figure 5A, **1** exhibited an inhibitory effect on HGF-induced cell scattering of MDCK cells in a dose-dependent manner. At the dose of 10 μM, the compound completely blocked cell spreading, as evidenced by the fact that MDCK cells remain in tight clusters.

1 Suppresses HGF-Induced Cell Migration. The cell scattering phenotype often requires the enhanced cell migratory ability. To examine the effect of **1** on cell motility, MDCK cells were treated with HGF in the presence of **1**, and the migratory ability was determined in vitro using a wound-healing assay. As shown in Figure 5B, **1** strongly suppressed HGF-induced cell motility in a dose-dependent manner and was sufficient to block the movement of most cells at a dose of 10 μM.

1 Reduces HGF-Induced Urokinase Activity. In addition to the elevated cell mobility, cancer invasiveness and metastasis require the degradation of the surrounding extracellular matrix by proteolytic enzymes, among which the serine protease urokinase is a key player. Moreover, urokinase is commonly up-regulated upon HGF stimulation.[16] To test the effect of **1** on HGF-induced urokinase up-regulation, the MDCK cells were treated with different concentrations of **1** in the presence of HGF. The tests showed that **1** inhibited HGF-induced urokinase activity in a dose-dependent manner and reached 80% inhibition at 10 μM (Figure 5C), suggesting that **1** suppresses cell invasion through the inhibition of urokinase up-regulation by HGF simulation.

1 Impairs HGF-Induced Branching Morphogenesis. HGF characteristically induces branching morphogenesis in certain Met-expressing cell lines when cultured in 3D collagen,[17] which presents another indicator of invasive potential. To determine the effect of **1** treatment on branching morphogenesis, MDCK cells were seeded within a three-dimensional matrix. As expected, only round cysts were observed in MDCK cells in the absence of HGF, whereas the cells formed multicellular-branched structures in the presence of HGF (Figure 5D). Exposure to **1** was sufficient to inhibit branching morphogenesis in MDCK cells (Figure 5D), indicating that **1** suppressed HGF-dependent invasive branched phenotype.

dx.doi.org/10.1021/jm3007454 | J. Med. Chem. 2012, 55, 8183–8187

Taken together, **1** inhibits HGF/c-Met axis and further inhibits HGF-stimulated cell metastatic behaviors.

The SAR Study on the Inhibition of HGF/c-Met Axis. In a SAR study, the new compound **1** and six relevant known compounds **2**−**7** were tested for the effects on HGF/c-Met axis (Figure 6). Compounds **1** and **2** strongly inhibited HGF-induced c-Met phosphorylation at 5 μM, and compound **3** only had marginal inhibitory effect at this dosage, while the other compounds, either the sesquiterpenoid motifs **4** and **5** or the phloroglucinols **6** and **7**, had no effects on HGF-mediated c-Met phosphorylation. Observation of the structures of compounds **1**−**7** and their effects on HGF/c-Met axis allowed the outline of SAR for this compound class: (1) The coupling of a phloroglucinol and a sesquiterpenoid is essential for the activity, (2) the C-4 and C-7′ coupling (**1**) of a phloroglucinol and a sesquiterpenoid is better than those with a C-4/C-9′ coupling (**2** and **3**), (3) the stereochemistry at C-9′ of the C-4/C-9′ coupled compounds (**2** and **3**) will affect the activity, e.g., compound **2** with a 9′β-isobutyl was more stronger than compound **3** bearing an 9′α-isobutyl group.

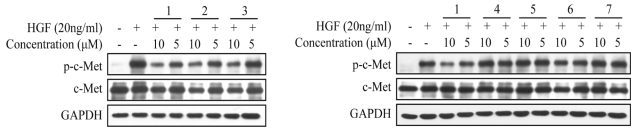

Figure 6. The effects of compounds **1**−**7** on HGF-induced c-Met phosphorylation.

CONCLUSION

In conclusion, **1** featured a new coupling pattern of phloroglucinol−sesquiterpenoid adducts, and in particular, it showed potent inhibition on HGF-induced c-Met activation and further suppressed HGF-stimulated cell motility and invasive behaviors. The novel structural architecture of **1** provided an opportunity for the development of a new class of HGF/c-Met axis inhibitors. The clear SAR outlined in the current study will facilitate the further structural modification of this compound class.

EXPERIMENTAL SECTION

Chemistry. The extraction and isolation of **1**−**7** were completed by solvent partition and extensive column chromatography (see SI for details).The purities (>95% or up) of **1**−**7** were checked by HPLC analysis with two different conditions (see SI for details).

Eucalyptin A (1). Pale-yellow amorphous powder; $[\alpha]_D^{20}$ −80.7 (*c* 0.545, MeOH). UV (MeOH) λ_{max} (log ε): 386 (4.87), 287 (4.65), 219 (4.62) nm. IR (KBr) ν_{max} 3425, 2955, 2926, 2870, 1616, 1460, 1375, 1309, 1186, 1604 cm^{-1}. ^{1}H NMR (400 MHz, $CDCl_3$): δ 10.09 (s, H-8′), 2.99 (m, H-10′), 2.82 (d, 14.2, H-7′ a), 2.26 (m, H-11′), 2.20 (m, H-7′ b), 2.04 (ddd, 8.9, 8.0, 4.6, H-1), 1.86 (m, H-8α), 1.76 (m, H-9β), 1.71 (m, H_2-2), 1.56 (m, H-9α), 1.46 (m, H_2-3), 1.17 (s, H_3-14), 1.11 (s, H_3-12), 1.06 (s, H_3-13), 1.09 (m, H-5), 0.99 (d, 6.4, H_3-12′ and H_3-13′), 0.89 (m, H-8β), 0.82 (s, H_3-15), 0.70 (m, H-7), 0.54 (t, 9.8, H-6). ^{13}C NMR (100 MHz, $CDCl_3$): δ 206.5 (C-9′), 192.0 (C-8′), 172.7 (C-1′), 168.0 (C-5′), 162.2 (C-3′), 104.6 (C-2′), 104.1 (C-4′), 103.4 (C-6′), 75.8 (C-10), 54.2 (C-1), 52.8 (C-10′), 48.0 (C-5), 46.8 (C-4), 44.2 (C-9), 40.4 (C-3), 32.2 (C-7′), 28.9 (C-12), 26.2 (C-6 and C-7), 25.0 (C-11′), 24.4 (C-2), 22.7 (C-12′ and C-13′), 20.2 (C-8 and C-14), 19.3 (C-11), 18.4 (C-15), 16.8 (C-13). EIMS (70 eV) *m*/*z* (%): 472 $[M]^+$ (4), 252 (24), 251 (43), 203 (100), 195 (10), 147 (12), 95 (124). ESIMS (positive) *m*/*z*: 495.2 $[M + Na]^+$, 455.2 $[M - H_2O + H]^+$. ESIMS (negative) *m*/*z*: 471.3 $[M - H]^-$. HREIMS *m*/*z*: 472.2853 $[M]^+$ (calcd for $C_{28}H_{40}O_6$, 472.2825).

Cell Culture. MDCK (Madin−Darby canine kidney epithelial cell), NCI-H441 (human lung papillary adenocarcinoma cell), and MKN-45 (human gastric adenocarcinoma cell) were cultured in RPMI 1640 medium, A549 (adenocarcinomic human alveolar basal epithelial cell) was cultured in F12 medium, and NIH-3T3/TPR-Met (mouse fibroblast cell stably express TPR-Met oncogene) were cultured in DMEM medium. DU-145 (human prostate carcinoma cell) was cultured in MEM medium. All medium were added with 10% fetal bovine serum. Cells were purchased from ATCC and maintained at 37 °C under 5% CO_2 atmosphere.

Western Blot Analysis. For MDCK, A549, NCI-H441, and DU145, cells were serum starved for 24 h and treated with increased concentration of the indicated compounds for 2 h at 37 °C and then incubated with the HGF for 15 min and lysed in 1× SDS sample buffer. For MKN-45 and NIH-3T3/TPR-Met, cells were treated with increased concentration of **1** for 2 h at 37 °C and then lysed in 1× SDS sample buffer. Those cell lysates were subsequently resolved on 10% SDS-PAGE, and transferred to nitrocellulose membranes. Membranes were probed with phospho c-Met and c-Met (all from Cell Signaling Technology) antibodies and then subsequently with HRP-conjugated anti-rabbit IgG. Immunoreactive proteins were detected using ECL Plus (GE Healthcare), and images were pictured by ImageQuant LAS 4010 (GE Healthcare).

Wound-Healing Assay. MDCK cells were seeded into 12-well plate and grown until formed a monolayer with 90% confluency. Cells were then scraped with a tip, and various concentrations of **1** and 50 ng/mL HGF were added to the appropriate wells. Pictures were then taken under microscope until total healing was observed in control well.

Cell Scattering Assay. MDCK cells (1.5 × 10^3 cells per well) were plated into 96-well plate and grown overnight. Increasing concentration of **1** and 50 ng/mL HGF were added to the appropriate wells and incubated at 37 °C, 5% CO_2 for 24 h. The cells were fixed with 4% paraformaldehyde for 15 min at room temperature and then stained by 0.2% violet purple, washed with water, and allowed to dry before taking photos. Pictures were taken under microscope.

uPA Assay. MDCK cells (1.5 × 10^3 cells per well) were plated in 96-well plate and grown overnight. Increasing concentration of **1** and 50 ng/mL HGF diluted with the fresh medium were added to the appropriate wells and incubated for 24 h. The plate was processed for determination of plasminogen activity by first rinsing wells twice with DMEM (without phenol red) and then adding 200 μL of reaction buffer [10% (v/v) 3 mM chromozym PL (Roche) in 100 mM glycine, 40% (v/v) 50 mM Tris pH 8.2, 50% (v/v) 0.05 unit/mL plasminogen (Roche) in DMEM (without phenol red), and 0.2% Tween-20] to each well. The plate was incubated at 37 °C, 5% CO_2 for 6 h before the absorbance of each well was read at 405 nm.

Cell Branching Morphogenesis. Cells at a density of 20000 cells/mL in RPMI 1640 medium were mixed with an equal volume of collagen I solution, plated at 0.1 mL/well of a 96-well culture plate, and incubated for 45 min at 37 °C, 5% CO_2 to allow collagen gelling. Then 50 ng/mL HGF with or without **1** at various concentrations dissolved in the 100 μL of growth medium were then added to each well. The medium was replaced with fresh growth medium every 2 days. Pictures were taken under microscope after 5 days.

ASSOCIATED CONTENT

Supporting Information

General methods, plant material, extraction and isolation, quantum chemical calculation of the ECD, ^{1}H-, ^{13}C NMR, ^{1}H−^{1}H COSY, HSQC, HMBC, ROESY, ESIMS, and IR spectra of **1** and the purity check of **1**−**7**. This material is available free of charge via the Internet at http://pubs.acs.org.

AUTHOR INFORMATION

Corresponding Author

*For M.Y.G.: phone, 86-21-50806072; fax, 86-21-50806072; E-mail, mygeng@mail.shcnc.ac.cn. For J.M.Y.: phone, 86-21-

50806718; fax, 86-21-50807088; E-mail, jmyue@mail.shcnc.ac.cn.

Author Contributions

[§]These authors contributed equally.

Notes

The authors declare no competing financial interest.

■ ACKNOWLEDGMENTS

Financial support of the National Natural Science Foundation (81102461, 81021062), and National Science & Technology Major Project "Key New Drug Creation and Manufacturing Program" (2011ZX09307-002-03 and 2012ZX09301-001-007) of China. We thank Prof. Y. K. Xu of Xishuangbanna Tropical Botanical Garden, CAS for the identification of this plant material.

■ ABBREVIATIONS USED

HGF, hepatocyte growth factor; SAR, structure activity relationship; ECD, electronic circular dichroism; RPMI, Roswell Park Memorial Institute; DMEM, Dulbecco's Modified Eagle Medium; MEM, minimum essential media; ATCC, American Type Culture Collection; uPA, urokinase-type plasminogen actvator

■ REFERENCES

(1) (a) Giordano, S.; Ponzetto, C.; Di Renzo, M. F.; Cooper, C. S.; Comoglio, P. M. Tyrosine kinase receptor indistinguishable from the c-*met* protein. *Nature* **1989**, *339*, 155−156. (b) Birchmeier, C.; Birchmeier, W.; Gherardi, E.; Vande Woude, G. F. Met, metastasis, motility and more. *Nature Rev. Mol. Cell Biol.* **2003**, *4*, 915−925. (c) Longati, P.; Comoglio, P. M.; Bardelli, A. Receptor tyrosine kinases as therapeutic targets: the model of the MET oncogene. *Curr. Drug Targets* **2001**, *2*, 41−55.

(2) (a) Dai, Y.; Siemann, D. W. BMS-777607, a small-molecule Met kinase inhibitor, suppresses hepatocyte growth factor-stimulated prostate cancer metastatic phenotype in vitro. *Mol. Cancer Ther.* **2010**, *9*, 1554−1561. (b) Comoglio, P. M.; Giordano, S.; Trusolino, L. Drug development of MET inhibitors: targeting oncogene addiction and expedience. *Nature Rev. Drug Discovery* **2008**, *7*, 504−516. (c) Lesko, E.; Majka, M. The biological role of HGF−MET axis in tumor growth and development of metastasis. *Front. Biosci.* **2008**, *13*, 1271−1280. (d) Matsumoto, K.; Nakamura, T. Hepatocyte growth factor and the Met system as a mediator of tumor−stromal interactions. *Int. J. Cancer* **2006**, *119*, 477−483.

(3) Zeng, J. F.; Liu, S. Q. In *Chinese Flora (Zhongguo Zhiwu Zhi)*; Science Press: Beijing, 1984; Vol. *53*, Chapter 1, pp 31−52.

(4) Yin, S.; Xue, J. J.; Fan, C. Q.; Miao, Z. H.; Ding, J.; Yue, J. M. Eucalyptals A−C with a new skeleton isolated from *Eucalyptus globulus*. *Org. Lett.* **2007**, *9*, 5549−5552.

(5) Ghisalberti, E. L. Bioactive acylphloroglucinol derivatives from *Eucalyptus* species. *Phytochemistry* **1996**, *41*, 7−22.

(6) Nishizawa, M.; Emura, M.; Kan, Y.; Yamada, H.; Ogawa, K.; Hamanaka, N. Macrocarpals: HIV-RTase inhibitors of *Eucalyptus globulus*. *Tetrahedron Lett.* **1992**, *33*, 2983−2986.

(7) (a) Kozuka, M.; Sawada, T.; Kasahara, F.; Mizuta, E.; Amano, T.; Komiya, T.; Goto, M. The granulation-inhibiting principles from *Eucalyptus globulus* LABILL. II. The structures of euglobal -Ia_1, -Ia_2, -Ib, -Ic, -IIa, -IIb and -IIc. *Chem. Pharm. Bull.* **1982**, *30*, 1952−1963. (b) Kozuka, M.; Sawada, T.; Mizuta, E.; Kasahara, F.; Amano, T.; Komiya, T.; Goto, M. The granulation-inhibiting principles from *Eucalyptus globulus* LABILL. III. The structures of euglobal-III, -IVb and -VII. *Chem. Pharm. Bull.* **1982**, *30*, 1964−1973.

(8) (a) Takasaki, M.; Konoshima, T.; Fujitani, K.; Yoshida, S.; Nishimura, H.; Tokuda, H.; Nishino, H.; Iwashima, A.; Kozuka, M. Inhibitors of skin-tumor promotion. VIII. Inhibitory effects of euglobals and their related compounds on Epstein−Barr virus activation (1). *Chem. Pharm. Bull.* **1990**, *38*, 2737−2739. (b) Umehara, K.; Singh, I. P.; Etoh, H.; Takasaki, M.; Konoshima, T. Five phloroglucinol−monoterpene adducts from *Eucalyptus grandis*. *Phytochemistry* **1998**, *49*, 1699−1704. (c) Osawa, K.; Yasuda, H.; Morita, H.; Takeya, K.; Itokawa, H. Macrocarpals H, I, and J from the leaves of *Eucalyptus globulus*. *J. Nat. Prod.* **1996**, *59*, 823−827.

(9) Crow, W. D.; Osawa, T.; Paton, D. M.; Willing, R. R. Structure of grandinol: a novel root inhibitor from *Eucalytus grandis*. *Tetrahedron Lett.* **1977**, *12*, 1073−1074.

(10) Kokumai, M.; Konoshima, T.; Kozuka, M.; Haruna, M.; Ito, K. Euglobal T1, a new euglobal from *Eucalyptus tereticornis*. *J. Nat. Prod.* **1991**, *54*, 1082−1086.

(11) Murata, M.; Yamakoshi, Y.; Homma, S.; Aida, K.; Hori, K.; Ohashi, Y. Macrocarpal A, a novel antibacterial compound from *Eucalyptus macrocarpa*. *Agric. Biol. Chem.* **1990**, *54*, 3221−3226.

(12) Diedrich, C.; Grimme, S. Systematic Investigation of Modern Quantum Chemical Methods to Predict Electronic Circular Dichroism Spectra. *J. Phys. Chem. A* **2003**, *107*, 2524−2539.

(13) Faure, R.; Ramanoelina, A. R. P.; Rakotonirainy, O.; Bianchini, J.-P.; Gaydou, E. M. Two-dimensional nuclear magnetic resonance of sesquiterpenes. 4. Application to complete assignment of proton and carbon-13 NMR spectra of some aromadendrane derivatives. *Magn. Reson. Chem.* **1991**, *29* (9), 969−971.

(14) (a) Beechan, C. M.; Djerassi, C. Terpenoids—LXXIV: The sesquiterpenes from the soft coral *Sinularia mayi*. *Tetrahedron* **1978**, *34*, 2503−2508. (b) Nagashima, F.; Tanaka, H.; Toyota, M.; Hashimoto, T.; Kan, Y.; Takaoka, S.; Tori, M.; Asakawa, Y. Sesqui- and diterpenoids from *Plagiochila* species. *Phytochemistry* **1994**, *36*, 1425−1430.

(15) Boland, D. J.; Brophy, J. J.; Fookes, C. J. R. Jensenone, a ketone from *Eucalyptus jensenii*. *Phytochemistry* **1992**, *31*, 2178−2179.

(16) Webb, C. P.; Hose, C. D.; Koochekpour, S.; Jeffers, M.; Oskarsson, M.; Sausville, E.; Monks, A.; Vande Woude, G. F. The geldanamycins are potent inhibitors of the hepatocyte growth factor/scatter factor−met-urokinase plasminogen activator−plasmin proteolytic network. *Cancer Res.* **2000**, *60*, 342−349.

(17) Zhang, Y. W.; Vande Woude, G. F. HGF/SF-met signaling in the control of branching morphogenesis and invasion. *J. Cell Biochem.* **2003**, *88*, 408−417.